Journal of Analytical Science and Technology

RESEARCH ARTICLE

Open Access

Detection of bladder tumor cells using motion features in urine

Minsuk Kim[1*]

Abstract

Urinary exfoliated tumor cells have emerged as promising biomarkers for predicting, diagnosing, and guiding therapy in bladder cancer. Several methodologies based on biological and physical differences between normal cells and malignant tumor cells have been developed over the past few years. However, these methods still did not have sufficient sensitivity or specificity. In this study, a remote analysis protocol was devised utilizing motion microscopy. This technique amplifies vibrations within a recorded video by re-rendering motions, thereby generating highly magnified visuals. This approach aims to detect dynamic motions that may not be perceptible to the human eye under normal observation. Remarkably, motion microscopy unveiled discernible fluctuations surrounding bladder malignant tumor cells, which we referred to herein as cellular trail. The cellular trails were predominantly evident at around 1 Hz in amplified video images, with a velocity of 22 μm/s. Moreover, cellular trails were observed regardless of whether they were in a non-Newtonian or Newtonian fluid environment. Significantly, this phenomenon was distinguishable even in urine samples. In conclusion, we suggest motion microscopy as an innovative approach for detecting urinary malignant tumors with potential clinical utility as a complementary tool to cytology.

Keywords Microfluidic system, Motion microscopy, Bladder carcinoma, Computational tool, Vibration

Introduction

Urothelial bladder carcinoma comprises the majority of bladder cancer cases and ranks as the second leading cause of mortality, accounting for an estimated 150,000 deaths annually (Jemal 2011). Hence, individuals with bladder cancer need persistent screening, depending on cytology and cystoscopy with tissue biopsies as the primary detection tools (Tilki et al. 2011). However, the challenges of low sensitivity and high variability in cytology with the high degree of invasiveness are major issues for diagnosis (van Rhijn et al. 2009). Therefore, a noninvasive technique for a rapid and precise detection of bladder carcinoma is highly desired. Urinary exfoliated malignant tumor cells have been used as a diagnostic marker in bladder cancer for decades (de Oliveira et al. 2020; Bhat and Ritch 2019). To capture urinary exfoliated malignant tumor cells, several techniques have been used and applied (Wu et al. 2023; Hayashi et al. 2020). These techniques are composed of density-based separation, microfilters, immunoaffinity, microfluidic sorting, or combination of these methods (Tilki et al. 2011; Ng et al. 2021; Harouaka et al. 2014). A recent technology based on microfluidic system uses deterministic lateral displacement with continuous high throughput to separate urothelial malignant tumor cells from urine (Chen et al. 2018). To develop a more convenient method, we have developed and reported a novel method to visualize specific microvibration of malignant tumor cells in continuous flow (Kim et al. 2020). Motion microscopy creates new images in a way that enhances the motions enough to be perceptible to the human eye (Wadhwa et al. 2017; Hurlburt and Jaffey 2015; Sellon et al. 2015). The principle is to magnify the subtle motion signals stored in each

*Correspondence:
Minsuk Kim
ms@ewha.ac.kr
[1] Department of Pharmacology, Inflammation-Cancer Microenvironment Research Center, College of Medicine, Ewha Womans University, Magokdong-ro 2-gil, Gangseogu, Seoul 07804, Republic of Korea

pixel of a digital image. Therefore, better amplification signals for specific frequencies can be generated with a higher number of pixels in a digital image (Wadhwa et al. 2017). Spatial local phase information was combined in different sub-bands of frames for each pixel at location (x, y), time t, scale r, and orientation θ using squares objective function (Wadhwa et al. 2017; Hurlburt and Jaffey 2015; Kim et al. 2020), $\underset{u,v}{\operatorname{argmin}} \sum_{i} A_{ri,\theta i}^{2} \left[\left(\frac{\partial_{ri,\theta i}}{x}, \frac{\partial_{ri,\theta i}}{y} \right)(u,v) - \Delta\phi_{ri,\theta i} \right]^{2}$. In a previous study, we were able to differentiate breast malignant tumor cells from blood using motion microscopy (Kim et al. 2020). This phenomenon was attributed to fluid friction induced by the roughness on the surface of malignant tumor cells. In this study, we hypothesized that the surface of bladder malignant tumor cells might also increase fluid resistance. Therefore, we conducted experiments using motion microscopy to investigate the potential of detecting tumor cells in urine.

Materials and methods

Cell culture

The SV-HUC-1 cells (ATCC, CRL-9520, USA) or bladder carcinoma 5637 (ATCC, HTB-9, USA) were cultured in RPMI 1640 (A2494201, Gibco, USA) supplemented with 10% heat-inactivated fetal bovine serum (A3160401, Gibco, USA), 2 mM glutamine, 20 mM Hepes (pH 7.5) and maintained at 37℃ under an atmosphere of 95% O_2 and 5% CO_2. Urothelial cells were obtained using a screen cell cytometer (ScreenCell, CY4FC, UK) from urine. 40 ml of urine for each sample was treated with imidazolidinyl urea (I5133, Sigma-Aldrich, USA; 20 g/L of total volume) and stored at 4 °C. Human urine samples were obtained from individuals with bladder cancer (UETC008C-BLCA UETC, *N* = *18*, BIOIVT, USA) or normal control group (HUMANURINE-0101417, *N* = *18*, BIOIVT, USA) using institutional review board (IBR)-approved consent forms and protocols.

Experimental procedures of motion microscope and microfluidic device

Urinary exfoliated cells were introduced to microfluidic device at a flow rate of 22 μm/s, and images were recorded through microscope at 1024 × 576 pixels and 900 frames per second. The recorded images were uploaded to lambda vue (https://lambda.qrilab.com/site/), and magnification was done with amplification ratio of 35 and wavelength from 0.1 to 10 Hz. Microfluidic devices (Microfit, South Korea) were placed on the stage of the microscope, and the fluid flow was controlled by individual syringe pumps (BS-9000–12, Braintree scientific, USA).

Quantification of cellular vibration intensity

The obtained images were subtracted through the rolling ball radius method, and cellular trails were individually selected. The area of histograms was quantified by ImageJ (Java-based image processing and analysis software). Data were acquired as arbitrary area values.

Measurement of viscosity

Hyaluronic acid (75,043, Sigma-Aldrich, USA) was slowly mixed with PBS (10,010,023, Gibco, USA) until completely liquefied. Viscosity was measured with a plate digital viscometer (ASTM D4287, Industrial physics Inks & coatings, the Netherlands), and shear rates were generated by rotating brush.

Fluorescence microscope

Briefly, urothelial cells were placed in 10% formalin for 3 h and incubated with antisera against FITC-conjugated CD47 (1:400; ab300124, abcam, USA). After washing with PBS, cells were visualized using Zeiss LSM 510 confocal microscope (Carl Zeiss, German).

Bladder tumor antigen and nuclear matrix protein 22

The urine sample is also analyzed with bladder tumor antigen stat (21-000-131, Polymedco, USA) and nuclear matrix protein 22 BladderChek (ALERE NMP22, Abbott, USA). Briefly, 3 drops of fresh urine are added to kits and allowed for a room temperature reaction for 30 min. In both tests, a positive result is determined when two distinct lines appear in both the target and control zones, while a negative result is indicated by the presence of only the control line.

Statistical analysis

Values are means ± SE. The significance of differences was determined by a two-way analysis of variance (ANOVA), or a one-way ANOVA followed by a Bonferroni post hoc analysis where appropriate. Differences were considered significant when $P < 0.05$.

Results and discussion

Design of cellular vibration analysis

Urothelial cells were obtained through filtration from urine, and experiments were subsequently conducted. To address the focusing issues arising from the different phases of multiple cells, we employed microfluidics to induce cell rolling on the surface. Urothelial cells were flowed through a polydimethylsiloxane-based microfluidic channel at a flow rate of 22 μm/s. Subsequently, the

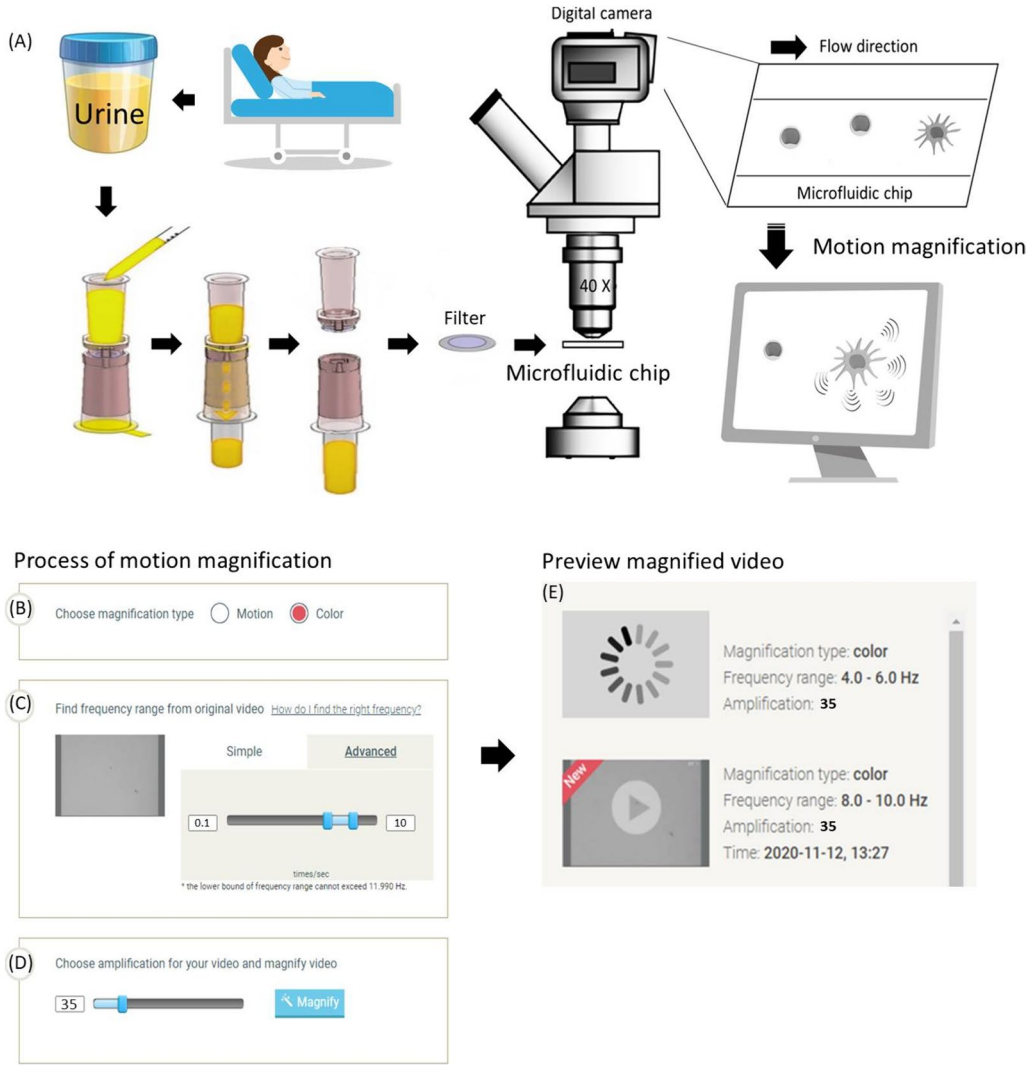

Fig. 1 Contact-free detection system to measure cellular vibration. **A** Schemata of the experimental setup of microfluidic device and motion microscope. Urothelial cells were obtained using a screen cell cytometer from urine. The cells were subjected to the microfluidic device at a flow rate of 22 µm/s, and video recording files were obtained from the microscope at 1024 × 576 pixels at 600 frames per second. Motion microscope amplified micromotions by video using spatial local phase. **B** The obtained videos were entered at lambda vue, and color modes were selected in magnification type. After setting the wavelength between 0.1 and 10 Hz (**C**), cellular vibrations were amplified 35 times (**D**) and magnified images were obtained (**E**)

cells were recorded at a frame rate of 600 per second with an image resolution of 1024 × 576 pixels (Fig. 1A). Cellular movements were amplified by a motion microscope, with detailed settings including color mode and magnification type (Fig. 1B), a wavelength range of 0.1 to 10 Hz (Fig. 1C), and an amplification rate of 35 times (Fig. 1D). The modified images were obtained through the outlined process (Fig. 1E).

Vibration of bladder malignant tumor cells according to wavelengths

Due to the reported diverse vibrations of cancer cells ranging from 0.5 to 3 Hz (Nelson et al. 2017), the subtle movements of SV-HUC-1 (nonmalignant urothelial cells) or 5637 (bladder malignant tumor cells) were amplified using a motion microscope within the frequency range of 0.5 Hz to 10 Hz. Here, 1 Hz corresponds to 60 invisible repetitive movements over 60 s. Interestingly, distinctive cellular trails were prominently observed in 5637 cells, but not in SV-HUC-1 cells (Fig. 2A, B). The cellular trails began to appear

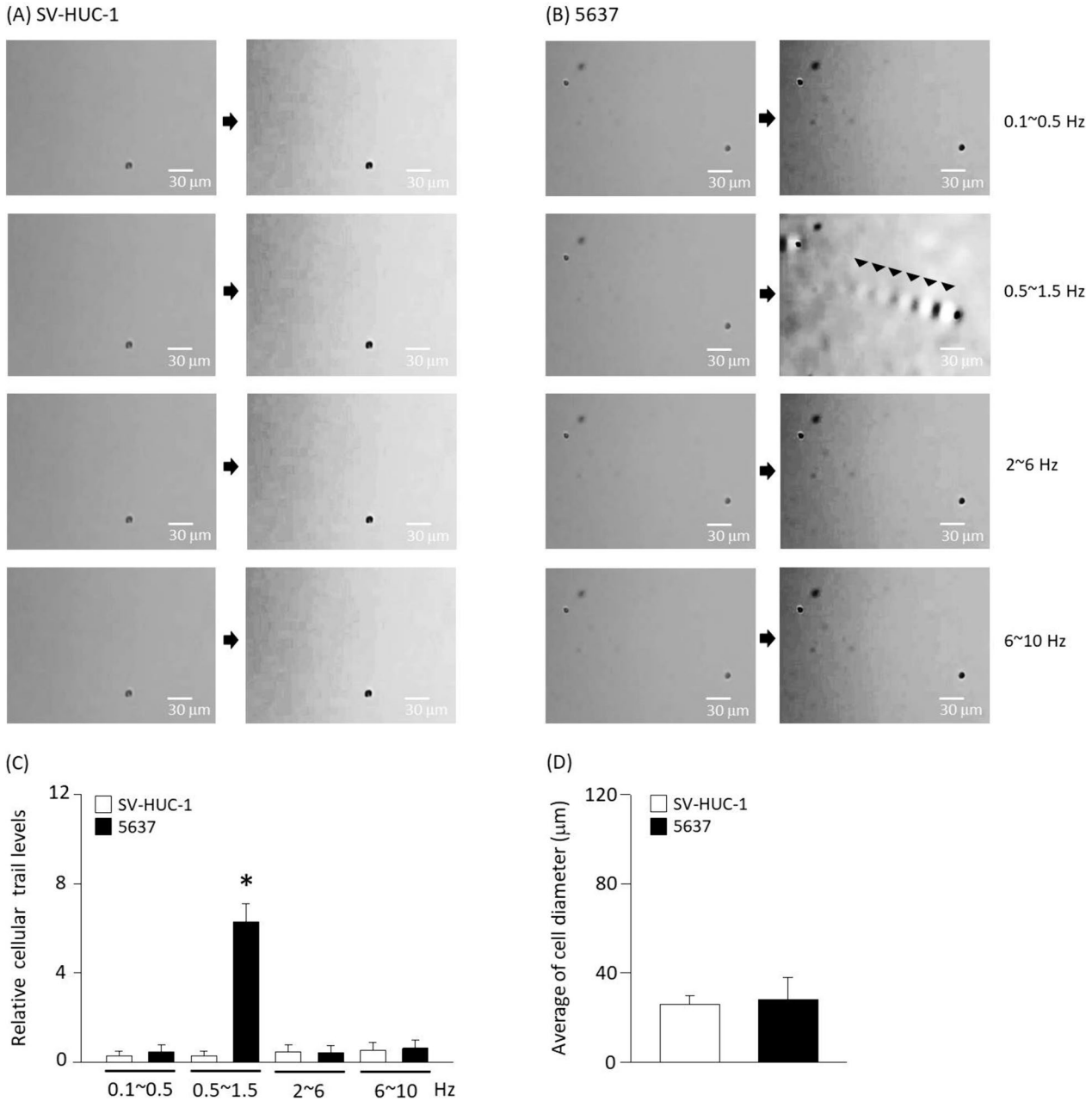

Fig. 2 Motion magnified video revealed cellular trail at 0.5–1.5 Hz. The images of microvibration of SV-HUC-1 (**A**) or 5637 (**B**) were converted by a motion microscope at 0.1 Hz to 10 Hz. 5637 showed distinct cellular trails (arrow heads) between 0.5 and 1.5 Hz. **C** Intensity levels of cellular trails in motion magnified videos between 0.5 and 1.5 Hz. **D** Diameters of urothelial cells. Results are the means ± SE of 6 experiments in each group. *Significantly different from motion magnified videos at 0.1–0.5 Hz, $P < 0.05$

from 0.5 Hz and eventually became challenging to detect from 2 to 10 Hz (Fig. 2C). There was no notable difference in the size of SV-HUC-1 or 5637 cells (Fig. 2D). Based on these findings, it was possible to differentiate tumor cells from urothelial cells regardless of their size under the specified conditions.

Tumor cellular trails were even observed in the urine

To confirm the feasibility of analyzing urothelial cells directly from urine samples, microscopic vibrations of cells were observed in various solutions. Cellular trails of 5637 cells were compared in cell culture medium, urine, or hyaluronic acid (Fig. 3A). Better observation of microscopic vibrations in hyaluronic acid, a type of

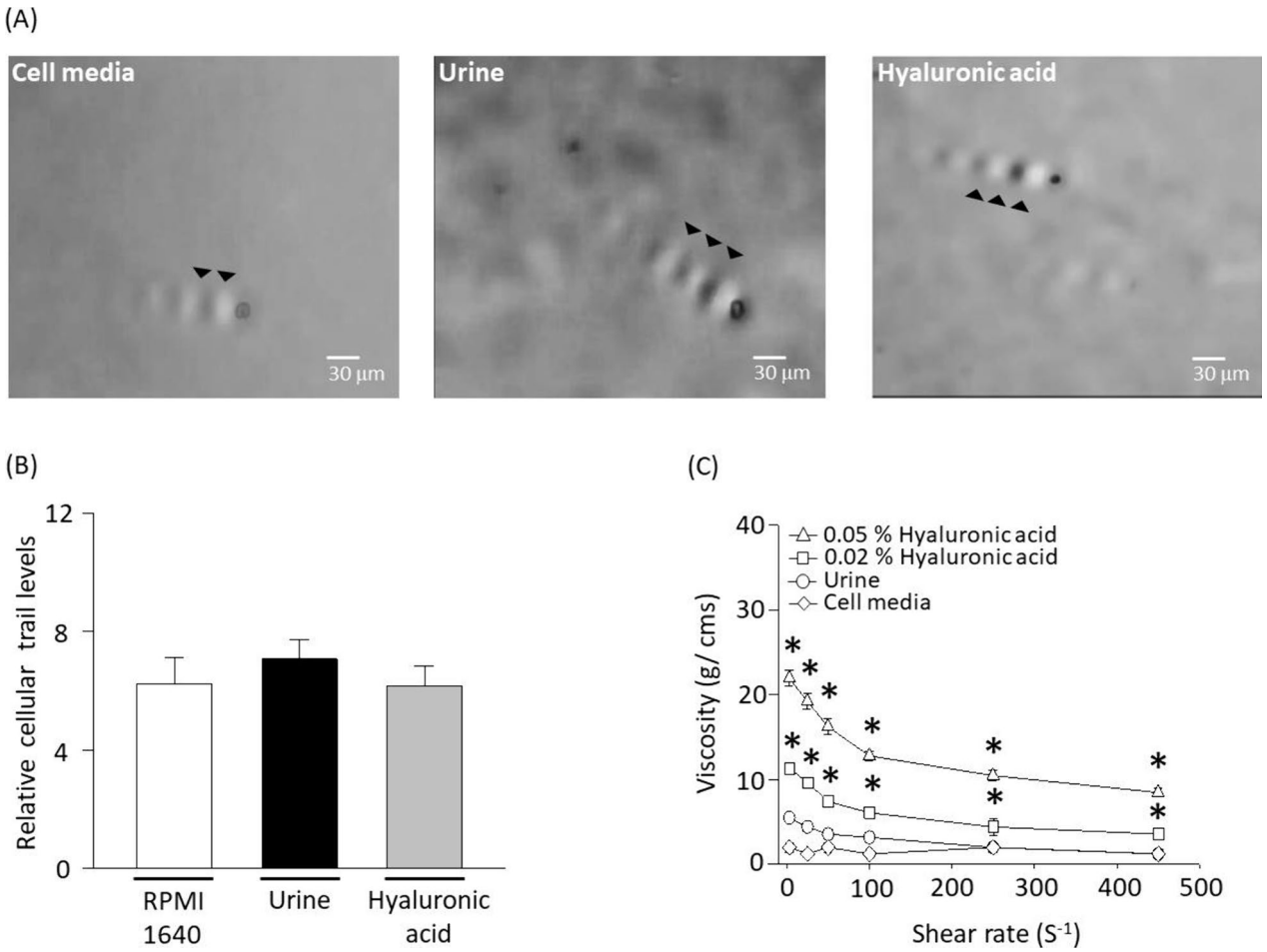

Fig. 3 Cellular trail in various solutions. **A** Cellular trails of 5637 were compared in cell culture medium (RPMI 1640), urine, or hyaluronic acid. **B** Intensity levels of cellular trails in motion magnified videos between 0.5 and 1.5 Hz. **C** Viscosity of hyaluronic acid was measured with a cone-and-plate digital viscometer at six different shear rates. The viscosity values for 0.02 and 0.05% hyaluronic acids were followed a pattern of a non-Newtonian fluid. Results are the means ± SE of 6 experiments in each group. *Significantly different from cell media treated group, $P < 0.05$

non-Newtonian fluid, had been reported (Park et al. 2022). However, there was no significant difference in the cellular trails using the various solutions (Fig. 3B). By measuring the viscosity of solutions based on shear stress, 0.02% and 0.05% hyaluronic acid exhibited non-Newtonian characteristics, while the cell culture medium and urine displayed Newtonian properties (Fig. 3C).

Motion microscope increases sensitivity of detecting bladder cancer

We next assessed human urine samples using motion microscope. Malignant tumor cells were stained with CD47 antibody and confirmed using fluorescence microscopy (Fig. 4A). We found that cellular trails can be clearly distinguished between malignant tumor cells and normal cells (Fig. 4B). The conventional urinary cytology and recently developed urine markers used for the clinical diagnosis of bladder cancer are often hampered by their limited sensitivity. To examine the performance of our motion microscope with other techniques, we compared it with bladder tumor antigen or nuclear matrix protein 22. The bladder tumor antigen or nuclear matrix protein 22 detection methods yielded a sensitivity of 67–78%, whereas motion microscopy method detected tumor cells with a sensitivity of 85–89% (Fig. 4C). It has not been known which part of the bladder tumor cells caused the microvibration. However, it has been reported that filopodia and extracellular matrix are related to fluid friction (Bera et al. 2022; Park et al. 2022) and linked to microvibrations on the cell surface (Park et al. 2022; Kim et al. 2020). The filopodia and extracellular matrix are frequently observed on the surface of bladder tumor cells. Overall, bladder malignant tumor cells were clearly distinguishable from normal urothelial cells using the motion microscope under condition of 22 μm/s and 0.5–1.5 Hz (Fig. 5). To clarify, further explanation is needed

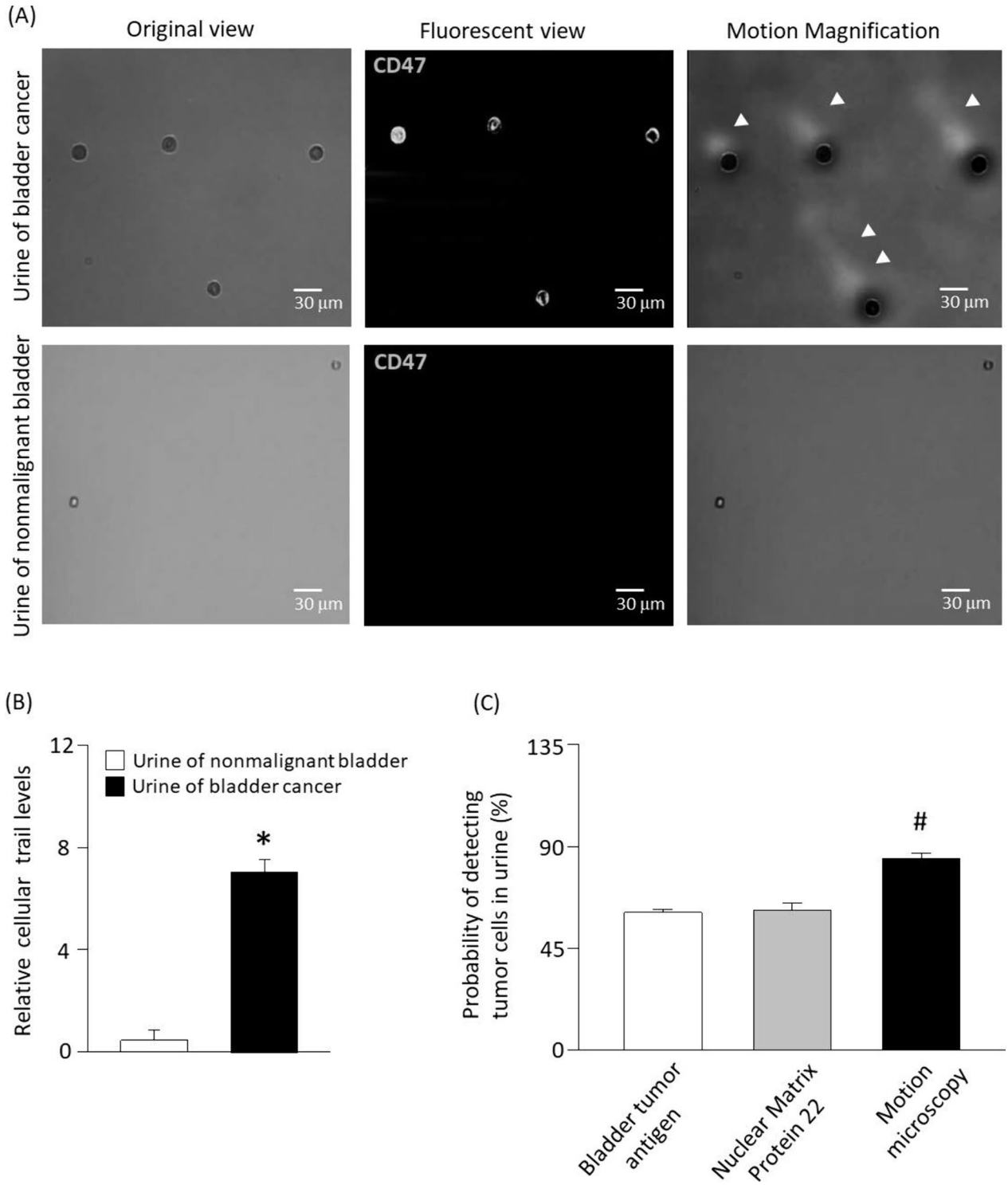

Fig. 4 Motion microscopy for bladder cancer detection. **A** Detection of bladder tumor cells by cellular trails in urine obtained from bladder cancer patients. Human bladder cancer cells were immunostained with CD47 antibody using fluorescence microscopy. The intensity level of cellular trails (arrows) was determined in motion magnified videos. **B** Intensity levels of cellular trails in motion microscopy. **C** Comparison with bladder tumor antigen, nuclear matrix protein 22 detection method, or motion microscope to detect bladder cancer cells in human urine samples. Results are the means ± SE of 6 experiments in each group. *Significantly different from cellular trail of nonmalignant cells, $P < 0.05$. #Significantly different from bladder tumor antigen method, $P < 0.05$

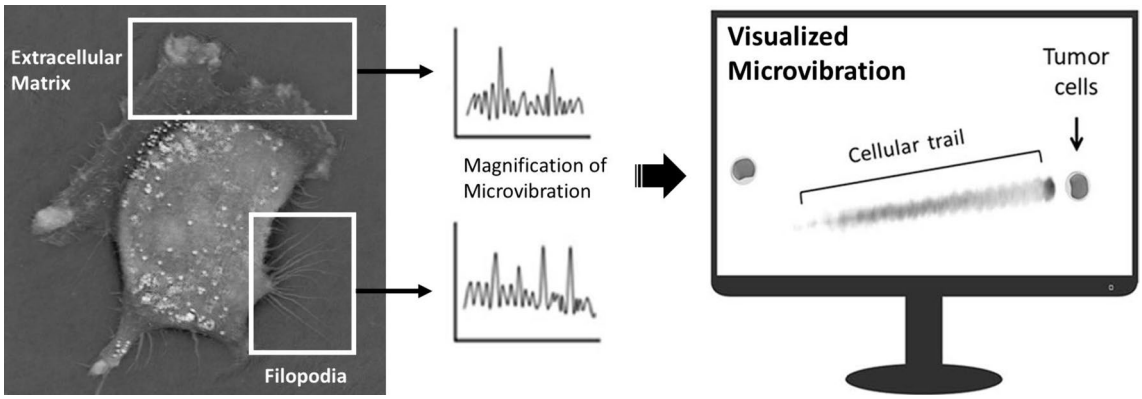

Fig. 5 Diagram of motion microscopy for bladder carcinoma detection. Motion microscope is able to detect oscillating movement of bladder tumor cells under condition of 22 μm/s and 0.5–1.5 Hz from human urine samples

on the principle behind the motion microscope detecting vibrations of cancer cells. Initially, it was understood that the vibrations of cancer cells were related to mitochondrial activity. However, there was no apparent connection between cellular vibration and mitochondria (Kim et al. 2020). The observation that these vibrations occurred only when cancer cells flowed through the solution led to the hypothesis that they were due to the physical properties of the cell surface rather than the interior of the cell (Kim et al. 2020). Experimental observation indicated that the surface of cancer cells had extracellular matrix and filopodia, which could easily induce fluid friction. Irregular shapes tend to induce fluid friction more effectively (Park et al. 2022).

Conclusion

The purpose of the current experiment is to develop diagnosis of urinary exfoliated tumor cells through visualization of microscopic vibrations. The presence or absence of malignant tumor cells was able to be confirmed through continuous video recording directly from the urine sample with higher sensitivity than conventional methods. Together, we offer a novel tool for detection of bladder cancer which may be used for assessment of drug efficacy with potential clinical utility.

Acknowledgements
We thank Minjeong Kim (Ewha medical student) for helping to culture tumor cells.

Author contributions
MK designed and performed experiments, analyzed data, prepared figures and wrote manuscript.

Funding
This work was supported by the National Research Foundation of Korea (NRF) Grant (2020R1A5A2019210 and 2019R1C1C1003384) funded by the Korean government (MSIT) and Ewha Womans University Research Grant of 2023.

Availability of data and materials
All data supporting the findings of this study are available within the paper.

Declarations

Ethics approval and consent to participate
The author is accountable for all aspects of the work in ensuring that questions related to the accuracy or integrity of any part of the work are appropriately investigated and resolved. This study was approved by the ethics committee and institutional review board of Ewha Womans University.

Consent for publication
The author read and approved the final version of the manuscript.

Competing interests
The author declares that they have no competing interests.

Received: 15 March 2024 Accepted: 3 June 2024
Published online: 10 June 2024

References

Bera K, Kiepas A, Godet I, Li YZ, Mehta P, Ifemembi B, Paul CD, Sen A, Serra SA, Stoletov K, Tao JX, Shatkin G, Lee SJ, Zhang YQ, Boen A, Mistriotis P, Gilkes DM, Lewis JD, Fan CM, Feinberg AP, Valverde MA, Sun SX, Konstantopoulos K. Extracellular fluid viscosity enhances cell migration and cancer dissemination. Nature. 2022;611(7935):365–73.
Bhat A, Ritch CR. Urinary biomarkers in bladder cancer: Where do we stand? Curr Opin Urol. 2019;29(3):203–9.
Chen AQ, Fu GH, Xu ZJ, Sun YK, Chen XY, Cheng KS, Neoh KH, Tang ZW, Chen SF, Liu M, Huang TX, Dai Y, Wang QB, Jin J, Jin BY, Han RPS. Detection of urothelial bladder carcinoma via microfluidic immunoassay and single-cell DNA copy-number alteration analysis of captured urinary-exfoliated tumor cells. Can Res. 2018;78(14):4073–85.
De Oliveira MC, Caires HR, Oliveira MJ, Fraga A, Vasconcelos MH, Ribeiro R. Urinary biomarkers in bladder cancer: where do we stand and potential role of extracellular vesicles. Cancers. 2020;12(6):1400–30.
Harouaka RA, Zhou MD, Yeh YT, Khan WJ, Das A, Liu X, Christ CC, Dicker DT, Baney TS, Kaifi JT, Belani CP, Truica CI, El-Deiry WS, Allerton JP, Zheng SY. Flexible micro spring array device for high-throughput enrichment of viable circulating tumor cells. Clin Chem. 2014;60(2):323–33.
Hayashi Y, Fujita K, Tomiyama E, Koh Y, Matsushita M, Nakano K, Ishizuya Y, Wang C, Kato T, Hatano K, Kawashima A, Ujike T, Uemura M, Nonomura N. Liquid biopsy analysis of TERT promoter mutation in urinary cell-free DNA in patients with urothelial carcinoma. J Urol. 2020;203:E928–9.

Hurlburt N, Jaffey S. A spectral optical flow method for determining velocities from digital imagery. Earth Sci Inf. 2015;8(4):959–65.
Jemal A. Global cancer statistics (vol 61, pg 69, 2011). CA Cancer J Clin. 2011;61(2):134–134.
Kim H, Ahn YH, Kim BS, Park S, Yoon JC, Park J, Moon CM, Ryu DR, Kang JL, Choi JH, Park EM, Lee KE, Woo M, Kim M. Motion microscopy for label-free detection of circulating breast tumor cells. Biosens Bioelectron. 2020;158:112131–9.
Nelson SL, Proctor DT, Ghasemloonia A, Lama S, Zareinia K, Ahn Y, Al-Saiedy MR, Green FHY, Amrein MW, Sutherland GR. Vibrational profiling of brain tumors and cells. Theranostics. 2017;7(9):2417–30.
Ng K, Stenzl A, Sharma A, Vasdev N. Urinary biomarkers in bladder cancer: a review of the current landscape and future directions. Urol Oncol Semin Orig Investig. 2021;39(1):41–51.
Park S, Kim H, Woo M, Kim M. Label-free detection of leukemic myeloblasts in hyaluronic acid. J Biol Eng. 2022;16(1):1629–38.
Sellon JB, Farrahi S, Ghaffari R, Freeman DM. Longitudinal spread of mechanical excitation through tectorial membrane traveling waves. Proc Natl Acad Sci USA. 2015;112(42):12968–73.
Tilki D, Burger M, Dalbagni G, Grossman HB, Hakenberg OW, Palou J, Reich O, Rouprêt M, Shariat SF, Zlotta AR. Urine markers for detection and surveillance of non-muscle-invasive bladder cancer. Eur Urol. 2011;60(3):484–92.
van Rhijn BWG, van der Poel HG, van der Kwast TH. Cytology and urinary markers for the diagnosis of bladder cancer. Eur Urol Suppl. 2009;8(7):536–41.
Wadhwa N, Chen JG, Sellon JB, Wei DL, Rubinstein M, Ghaffari R, Freeman DM, Büyüköztürk O, Wang P, Sun SJ, Kang SH, Bertoldi K, Durand F, Freeman WT. Motion microscopy for visualizing and quantifying small motions. Proc Natl Acad Sci USA. 2017;114(44):11639–44.
Wu SY, Li R, Jiang YH, Yu JZ, Zheng JY, Li ZY, Li MY, Xin KR, Wang Y, Xu ZQ, Li SJ, Chen XN. Liquid biopsy in urothelial carcinoma: detection techniques and clinical applications. Biomed Pharmacother. 2023;165:115027–58.

Publisher's Note